Chemical Science

ROYAL SOCIETY OF CHEMISTRY

EDGE ARTICLE

View Article Online
View Journal | View Issue

Cite this: *Chem. Sci.*, 2023, **14**, 9055

All publication charges for this article have been paid for by the Royal Society of Chemistry

Received 12th June 2023
Accepted 1st August 2023

DOI: 10.1039/d3sc02992a

rsc.li/chemical-science

Rhodium(I)-catalyzed cascade C(sp^2)–H bond alkylation – amidation of anilines: phosphorus as traceless directing group†

Marie Peng,[a] Denis Ari,[a] Thierry Roisnel,[a] Henri Doucet[a] and Jean-François Soulé *[b]

We introduce a versatile Rh(I)-catalyzed cascade reaction, combining C(sp^2)–H bond functionalization and amidation between *N*-arylphosphanamines and acrylates. This innovative approach enables the rapid synthesis of dihydroquinolinone scaffolds, a common heterocycle found in various pharmaceuticals. Notably, the presence of the phosphorus atom facilitates the aniline *ortho*-C(sp^2)–H bond activation prior to N–P bond hydrolysis, streamlining one-pot intramolecular amidation. Moreover, we demonstrate the applicability of this reaction by synthesizing an antipsychotic drug. Detailed mechanistic investigations revealed the involvement of a Rh–H intermediate, with substrate inhibition through catalyst saturation.

Introduction

Benzo-fused *N*-heterocycles are valuable bulling blocks in molecular sciences, including medicinal and materials chemistry. Remarkably, several drug leads feature dihydroquinolinone scaffolds (Fig. 1A).[1] For instance, carteolol is a non-selective beta blocker used to treat glaucoma; cilostazol is a medication used to help the symptoms of intermittent claudication in peripheral vascular disease, and vesnarinone is a cardiotonic agent. Dihydroquinolinones were formerly prepared from aniline derivatives *via* amidation reaction followed by intramolecular Friedel–Crafts reaction in the presence of an excess amount of Lewis acid, typically $AlCl_3$ (Fig. 1B, left).[2] Due to their importance, several strategies considering better process sustainability have been developed, ranging from transition metal-catalyzed cyclization reactions[3] and radical cyclizations.[4] Since these approaches require multi-step synthesis of the precursors and specific starting materials, they are often limited to preparing a few particular examples. On the other hand, a more direct approach for synthesizing dihydroquinolinones through the concomitant formation of C–C and C–N bonds, so-called C(sp^2)–H bond annulation remains unexplored (Fig. 1B, right). This approach is highly desirable as mere anilines and acrylates are the starting materials. However, this C(sp^2)–H bond annulation for the formation of dihydroquinolinones has proven to be incredibly challenging given the inherent nucleophilic characters of anilines which are prone to react in 1,4-addition reaction affording trisubstituted

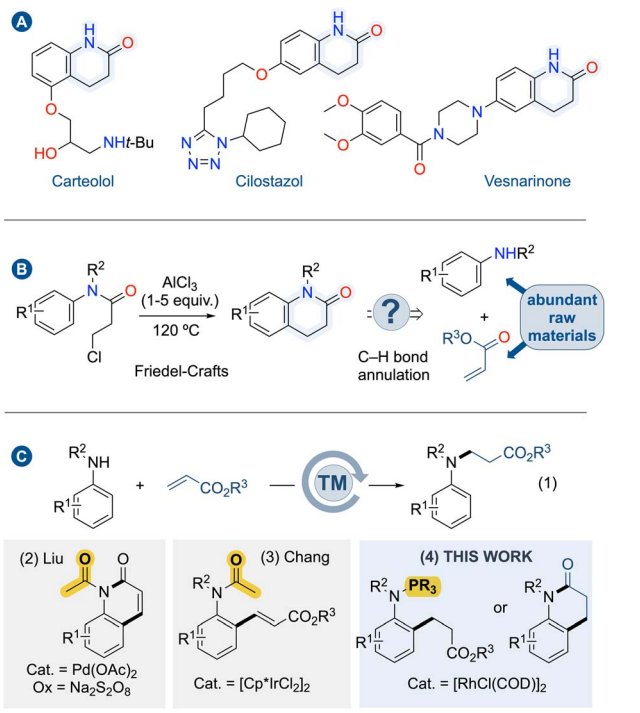

Fig. 1 Dihydroquinolinones & their preparation: (A) selected examples of dihydroquinolinones-containing drug leads. (B) Traditional synthesis of dihydroquinolinones *vs.* C(sp^2)–H bond annulation. (C) Key role of the directing group for anilines acrylates couplings: amination, alkenylation *vs.* alkylation.

[a]*Univ. Rennes, CNRS UMR6226, Rennes F-3500, France*

[b]*Chimie ParisTech, PSL University, CNRS, Institute of Chemistry for Life and Health Sciences, 75005 Paris, France. E-mail: jean-francois.soule@chimieparistech.psl.eu*

† Electronic supplementary information (ESI) available. CCDC 2252526. For ESI and crystallographic data in CIF or other electronic format see DOI: https://doi.org/10.1039/d3sc02992a

anilines (Fig. 1C(1)).[5] To swap the selectivity toward C(sp^2)–H bond functionalization at the *ortho*-position of the *N*-atom, a directing group (DG) has to be installed.

The second issue to face is the selectivity between alkenylation *versus* alkylation. For instance, in 2015, Liu and co-workers demonstrated that the installation of a transient acetamido as a directing group on aniline partners allows the synthesis of 2-quinolinones through a cascade reaction of Pd-catalyzed C(sp^2)–H alkenylation – cyclization reaction (Fig. 1C(2)).[6] Therefore, a subsequent hydrogenation step of the double bond is required to deliver dihydroquinolinones.[7] The alkenylation *versus* alkylation selectivity generally depends on the choice of the directing group. Indeed, Chang and co-workers demonstrated that the acetamido group affords alkenylation, while pyridine, pyrazole, and pyrimidine lead to alkylation products using [Cp*IrCl$_2$] catalyst (Fig. 1C(3)).[8] Nevertheless, utilizing Rh(III)-catalysis, the non-removable directing group of pyridine enables alkenylation even within the annulation process.[9] Alternatively, allylic alcohols can be used in Rh(III)-catalyzed *ortho*-directed C–H bond alkylations of anilines using pyrimidine as non-removable directing group.[10] Following the discovery that trivalent phosphorus [P(III)] acts as directing group for the C(sp^2)–H bond functionalization of phosphines[11] or indoles,[12] and given the fact that P(III) favors alkylation products with acrylates using Rh(I) catalysts,[13] we hypothesized that if *N*-arylphosphanamines could be alkylated at *ortho*-position with acrylates, such intermediate would rapidly undergo intramolecular amidation reaction driven by N–P bond hydrolysis provided that suitable conditions are found (Fig. 1C(4)). Herein, we describe the reaction development with mechanistic aspects showcasing that trivalent phosphorus acts as a traceless directing group in Rh(I)-catalyzed cascade reaction of C(sp^2)–H bond activation/alkylation – amidation of anilines with acrylate derivatives for the one-pot synthesis of dihydroquinolinones.

Table 1 Optimization of the reaction conditions

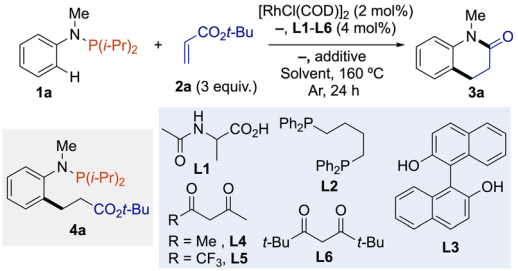

Entry	L	Additive	Solvent	**3a**[a] (%)
1	—	—	Toluene	42[b]
2	—	—	1,4-Dioxane	12[b]
3	—	—	$ClCH_2CH_2Cl$	24
4	—	—	DMF	40
5	—	NaOAc (0.3 equiv.)	DMF	30
6	—	$AlMe_3$ (0.2 equiv.)	DMF	20
7	**L1**	—	DMF	54
8	**L2**	—	DMF	36
9	**L3**	—	DMF	46
10	**L4**	—	DMF	45
11	**L5**	—	DMF	22
12	**L6**	—	DMF	58
13	**L6**	MS 4 Å (50 mg)	DMF	21 (51)[c]
14	**L6**	H_2O (2 equiv.)	DMF	62
15	**L6**	H_2O (6 equiv.)	DMF	75
16	**L6**	H_2O (10 equiv.)	DMF	90 (81)
17	**L6**	H_2O (20 equiv.)	DMF	54
18	—	H_2O (10 equiv.)	DMF	35
19[d]	**L6**	H_2O (10 equiv.)	DMF	85
20[e]	**L6**	H_2O (10 equiv.)	DMF	84

[a] Determined by GC-analysis using *n*-dodecane as internal standard, isolated yield is shown in parentheses. [b] Yield obtained after HCl hydrolysis. [c] Yield of **4a**. [d] Methyl acrylate instead of *tert*-butyl acrylate. [e] Ethyl acrylate instead of *tert*-butyl acrylate.

Results and discussion

To demonstrate the feasibility of the one-pot cascade of the C(sp^2)–H bond alkylation – amidation reaction, we carried out optimization with phosphanamine **1a** and *tert*-butylacrylate (**2a**) as the annulative agent. Using our previously published method for the C(sp^2)–H bond alkylation of phosphines as the starting point,[13a] we quickly recognized that the most important aspect of reaction optimization was identifying the optimal solvent (and additive) to promote C(sp^2)–H bond alkylation followed by the one-pot removal of P(i-Pr)$_2$ directing group to trigger amidation reaction and deliver the dihydroquinolin-2-one scaffold. Indeed, in toluene or 1,4-dioxane, desired product **3a** was obtained among intermediate **4a**, which could be converted into **3a** by acidic hydrolysis (Table 1, entries 1 and 2). In contrast, the one-pot process occurred in 1,2-dichloroethane or DMF, affording dihydroquinolin-2-one **3a** in 24% and 40% yield, respectively, without additional treatment (Table 1, entries 3 and 4). The addition of base to favor C(sp^2)–H bond cleavage,[14] or Lewis acid to promote the amination reaction (see ESI†) have both a negative effect on the reaction outcomes (Table 1, entries 5 and 6). Next, we examined the effect of ligands with the aim of increasing the reactivity. Protected amino-acid such as Ac-Ala (**L1**) slightly improved the reaction to afford **3a** in 54% yield, while diphosphine **L2** failed to affect the title reaction (Table 1, entries 7 and 8). Diols, such as BINOL (**L3**), previously employed by Shi in Rh(I)-catalyzed phosphine-directed C(sp^2)–H functionalization,[12b] did not gave better results (Table 1, entry 9). A set of bidentate acac-type ligands **L4–L6** was tested and 2,2,6,6-tetramethylheptane-3,5-dione (**L6**) was the most efficient, providing **3a** in 58% yield (Table 1, entries 10–12). However, the yield in **3a** varied when different qualities of solvents were employed. Nevertheless, the reaction proceeded to completion, resulting in the observation of a mixture containing both **3a** and **4a**, demonstrating the superiority of DMF. The **3a**/**4a** selectivity varaition may be due to the amount of water necessary to hydrolyze the *N*-arylphosphanamine into aniline derivatives. In the presence of molecular sieves, the reaction was much less effective and intermediate **4a** was obtained as the major product in 51%; while in the presence of a small amount of water, reproducible results were obtained, and 10 equivalents was the best stoichiometry affording **3a** in 81% isolated yield (Table 1, entries 13–17). Control experiment without **L6** but with 10

equivalents of water gave a lower yield of 35% in **1a**, revealing the importance of **L6** in the catalytic conditions (Table 1, entry 18). It is worth mentioning that reactions performed with methyl or ethyl acrylate gave **3a** in similar yields (Table 1, entries 19 and 20).

With the aforementioned optimal reaction conditions established, the substrate scopes of this reaction were then examined (Scheme 1). First, different substituents on the aromatic ring of the aniline moiety were examined. Electron-donating (MeO, Me) and electron-withdrawing (OCF_3, F, Cl) groups at the *para*-position of the *N*-atom were tolerated providing dihydroquinolinones **3b–f** in good to high yields. However, the conditions were incompatible with Br substituent on the *N*-arylphosphanamine partner. When *meta*-substituted phosphanamines were employed, the C(sp^2)–H bond alkylation regioselectivity occurred at the less hindered position, whatever the substituent, as exemplified by products **3h–k** containing F, Cl, Me, or MeO groups. From *N*-(3,5-difluorophenyl)-1,1-diisopropyl-*N*-methylphosphanamine, dihydroquinolinone **3l** was isolated in 72% yield. Reaction with *ortho*-fluoro-*N*-arylphosphanamine **1m** gave **3m** in a moderate yield of 42%. Other alkyl groups on the *N*-atom such as Et or *n*-Bu were also tolerated affording **3n–p** in 75–83% yields.[15] Beyond *N*-alkyl phosphanamines, 1,2,3,4-tetrahydroquinoline was also subjected to this C(sp^2)–H bond annulation to afford tricyclic amide **3q** in 70% yield. α-Substituted acrylates such as dimethyl 2-methylenesuccinate (**2b**) and methyl methacrylate (**2c**) were also successfully coupled with **1a** to produce 3-substituted *N*-methyl-dihydroquinolinones **3r** and **3s** in 57% and 60% yield, respectively.

Satisfied by these results, we then moved to extend this trivalent phosphorus traceless directing group strategy to *ortho*-C(sp^2)–H bond functionalization of anilines with styrene derivatives (Scheme 2). Accordingly, *ortho*-alkylated *N*-methyl aniline **5a** was obtained in 60% yield from **1a** and styrene (**2d**) using the same catalytic system, namely 2 mol% $[RhCl(COD)]_2$ associated with 4 mol% of **L6** in the presence of 10 equivalents of water in DMF. Noteworthy, the C–P bond was not fully hydrolyzed when the reaction was performed without water. Electron-rich 1-(*tert*-butyl)-4-vinylbenzene displayed a higher reactivity than styrene, as exemplified by forming **5b** and **5c** in 65% and 73% yield, respectively. This reactivity trend was also confirmed with 1-methoxy-4-vinylbenzene and 2,4-dimethyl-1-vinylbenzene, with which **1a** was coupled to give the *ortho*-alkylated *N*-methyl anilines **5d** and **5e** in 75% and 69% yield, respectively. Conversely, the reaction was more sluggish with styrenes holding an electron-withdrawing group such as F and Cl, as the resulting products **5f** and **5g** were isolated in only 32% and 42% yields.

Having established a method to construct dihydroquinolinones with good functional group compatibility, we investigated the feasibility of applying it to prepare aripiprazole *N*-methylated analog **8**. Aripiprazole treats schizophrenia, bipolar disorder, major depressive and tic disorders.[16] In 2020, the aripiprazole market was dominated by two brand companies (Otsuka & Bristol-Myers Squibb) and is expected to grow at a CAGR of 4.60% in the forecast period of 2022–2029. The majority of previous routes toward aripiprazole (or its *N*-alkyl congeners) involved multi-step synthesis for the construction of the dihydroquinolinone scaffold[17] (*e.g.*, intramolecular Friedel–Craft reaction followed by Pd-catalyzed hydrogenation of double bond,[18] or through a Beckmann rearrangement from indanone derivative). Owing to the increasing demand for aripiprazole and its *N*-alkyl analogs, and the lack of synthetic routes for the construction of dihydroquinolinones from simple starting materials prompted us to develop an efficient route to aripiprazole *N*-methylated analog **8**, employing our Rh(I)-catalyzed cascade

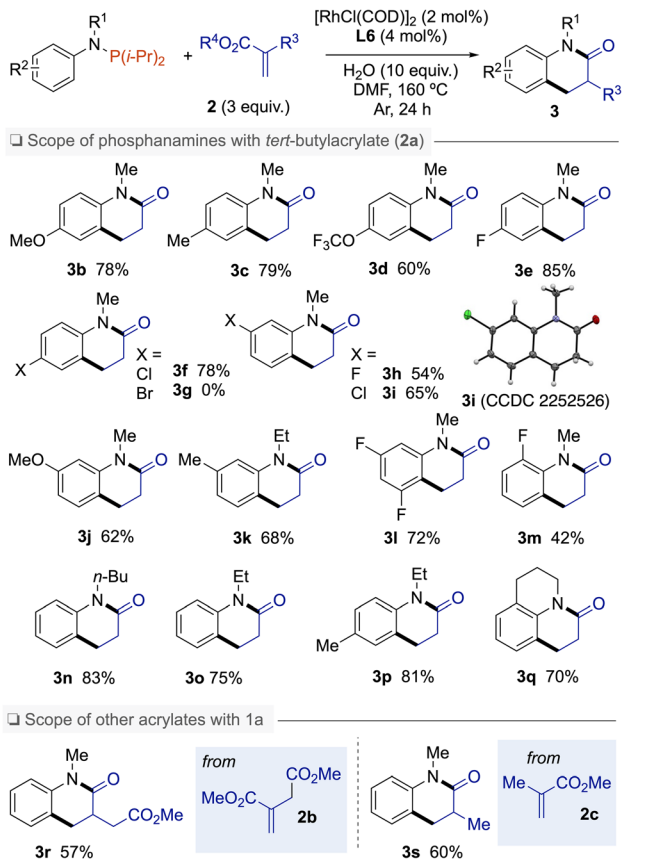

Scheme 1 Scope of the Rh(I)-catalyzed C–H bond activation with migrations of nitroarenes.

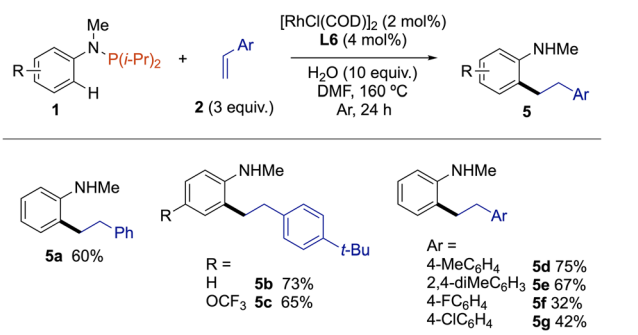

Scheme 2 Scope of C–H bond alkylation of *N*-arylphosphanamines with styrenes.

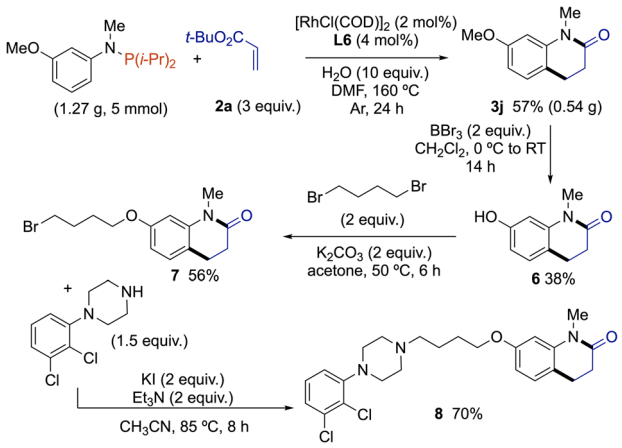

Scheme 3 Gram-scale reaction and synthesis of aripiprazole *N*-methylated analog.

reaction of C(sp^2)–H bond alkylation – amidation of anilines (Scheme 3). A gram-scale reaction (5 mmol) performed from 1,1-diisopropyl-*N*-(3-methoxyphenyl)-*N*-methylphosphanamine with **2a** gave 0.54 g of **3j** (57% yield). Then, classical deprotection of phenol group by BBr_3, followed by Williamson reaction using 2 equivalents of 1,4-dibromobutane in the presence of K_2CO_3 afforded **7** in good yield. Final coupling with 1-(2,3-dichlorophenyl)piperazine in the presence of KI as a relay-nucleofuge and triethylamine as base led to the formation of desired aripiprazole *N*-methylated analog **8** in 70% yield.

Intrigued by the exact role and the becoming of the phosphorus group along this reaction, we started a mechanistic investigation by carrying out a set of control experiments. No reaction occurred from *P*,*P*-diisopropyl-*N*-methyl-*N*-phenylphosphinic amide, indicating that trivalent phosphorus is not oxidized at least before the C(sp^2)–H bond cleavage. The use of classical acetamide as a directing group or reaction from *N*-methylaniline also failed to deliver cyclized amide **3a** (Fig. 2A). These results indicate that trivalent phosphorus is the active directing group. A standard reaction between phosphanamine **1a** and **2a** in the presence of 1 equivalent of 3-fluoro-*N*-methylaniline revealed that there is no phosphorus-directing group scrambling (Fig. 2B). A careful analysis of the reaction outcomes by GC-MS and ^{31}P NMR has allowed us to identify the formation

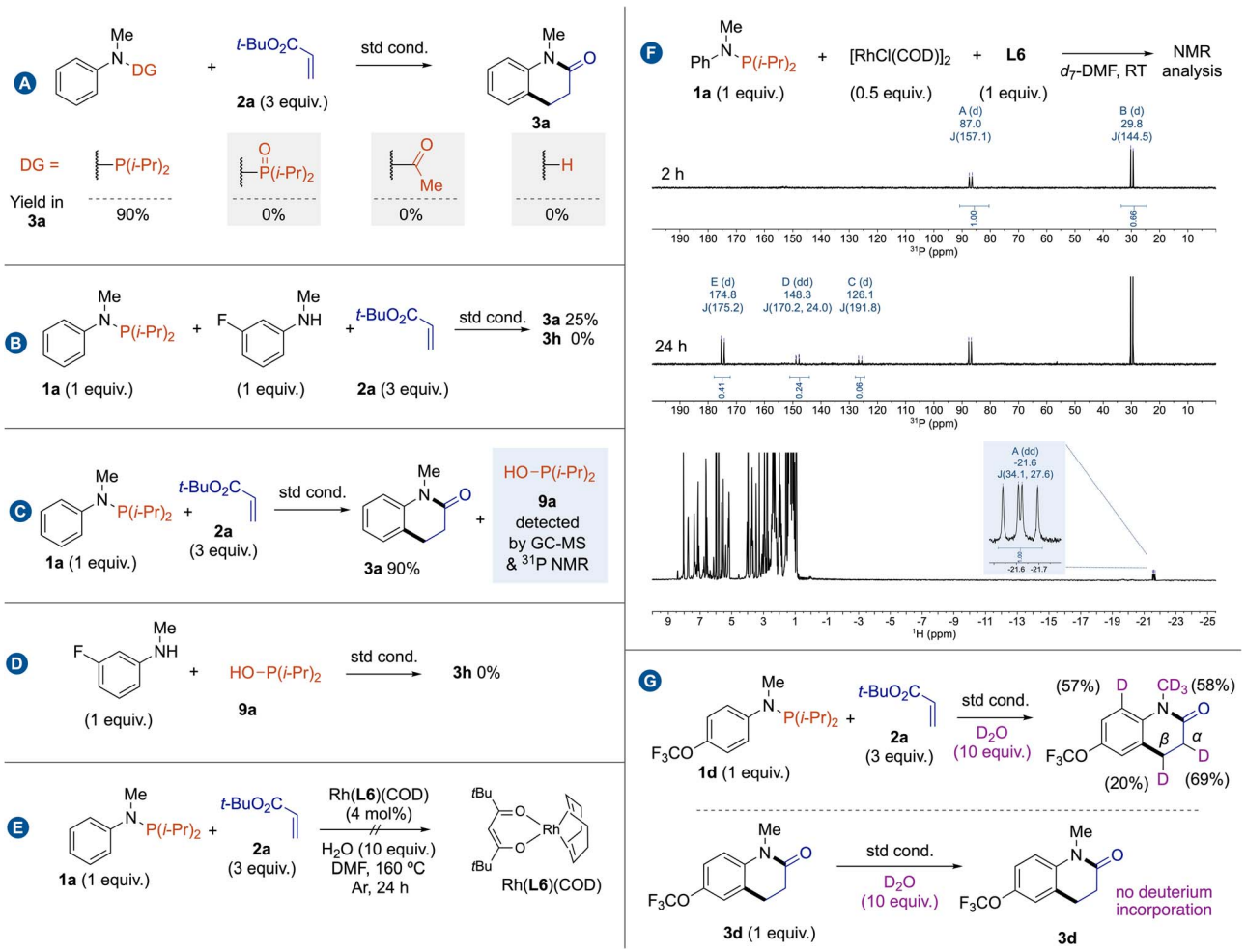

Fig. 2 Mechanistic studies: (A) control experiments using different directing groups, (B) parallel control experiment, (C) detection of residual phosphorus, (D) control experiment of the reactivity of NH amide substrate in the presence of **9a**, (E) reactivity of RhL6(COD) complex, (F) Stoichiometric reactions (G) deuterium labelling experiments.

hydroxydiisopropylphosphane (**9a**) as the side product,[19] which may explain that -P(i-Pr)$_2$ acts as a traceless directing group rather than a transient directing group (Fig. 2C).[20] To completely rule out the intermediacy of the NH amide substrate, we conducted a control experiment in the presence of one equivalent of **9a**, which did not yield the product **3a** (Fig. 2D). To determine the role of **L6**, we decided to prepare the well-defined Rh(**L6**)(COD) complex, but it was completely inactive for this cascade reaction (Fig. 2E). This result may suggest that **L6** has an indirect role, possibly in a catalyst regeneration process, by facilitating the decomplexation of **9a** through an unknown mechanism. To get more information on the structure of rhodium intermediates, we then conducted a stoichiometric reaction between [RhCl(COD)]$_2$ and **1a** with *in situ* following by NMR spectroscopies (Fig. 2F). At room temperature, a mixture of two distinct phosphorus containing Rh complexes was observed within two hours. It is generally accepted that treatment of complexes [{Rh-(COD)(μ^2-Cl)}$_2$] with phosphine ligands in the absence of silver salts smoothly affords neutral μ^2-bridged dinuclear rhodium complexes of the type [{Rh(phosphine)$_2$(μ^2-Cl)}$_2$].[21] The signal at 87.1 ppm (d, $^1J_{Rh,P}$ = 156.7 Hz) is attributed to [{Rh(**1a**)$_2$(μ^2-Cl)}$_2$]; while after isolation, we can attribute the signal at 30.4 ppm (d, $^1J_{Rh,P}$ = 140.5 Hz) to [{Rh(**9a**)$_2$(μ_2-Cl)}$_2$]. This complex might be formed through the *in situ* hydrolysis of P–N bond by water. After 24 h, the proportion of [{Rh(**9a**)$_2$(μ^2-Cl)}$_2$] increases, indicating that it is the resting state catalyst. Although multiple doublet signals are also observed by ^{31}P NMR data, a characteristic Rh–H signal appears as a doublet of doublets at −21.66 ppm ($^1J_{Rh,H}$ = 34.1 Hz, $^2J_{P,H}$ = 27.6 Hz) in ^{1}H NMR, proving that a C–H bond activation mechanism rather than a CMD mechanism (Fig. 2F). To gain further insight into the reaction mechanism, deuterated labelling experiments were carried out in the standard reaction conditions (Fig. 2G). A standard reaction performed using 10 equivalents of deuterated water gave 57% deuterium incorporation at *ortho*-position of the NMeP(i-Pr)$_2$ group. This deuterium labelling experiment suggests that the C(sp^2)–H bond cleavage is reversible. Moreover, 69% and 20% deuterium incorporations were detected at the α and β-positions of the ester group of **3d**. In addition, the deuterium incorporation in the NMe group may result from the formation of amide rhodacycle through C(sp^3)–H bond activation. The control experiment involving **3d** under deuterium labelling conditions does not show any deuterium incorporation in **3d**. The observed H/D isotopic exchanges likely occur due to the formation of Rh–D species, similar to a process described by Martin and Milstein in the C–H bond activation of benzylphosphine by Rh(I) complexes.[22] Furthermore, the incorporation of deuterium at the α-position of the ester group should result from an insertion/β-H elimination process.

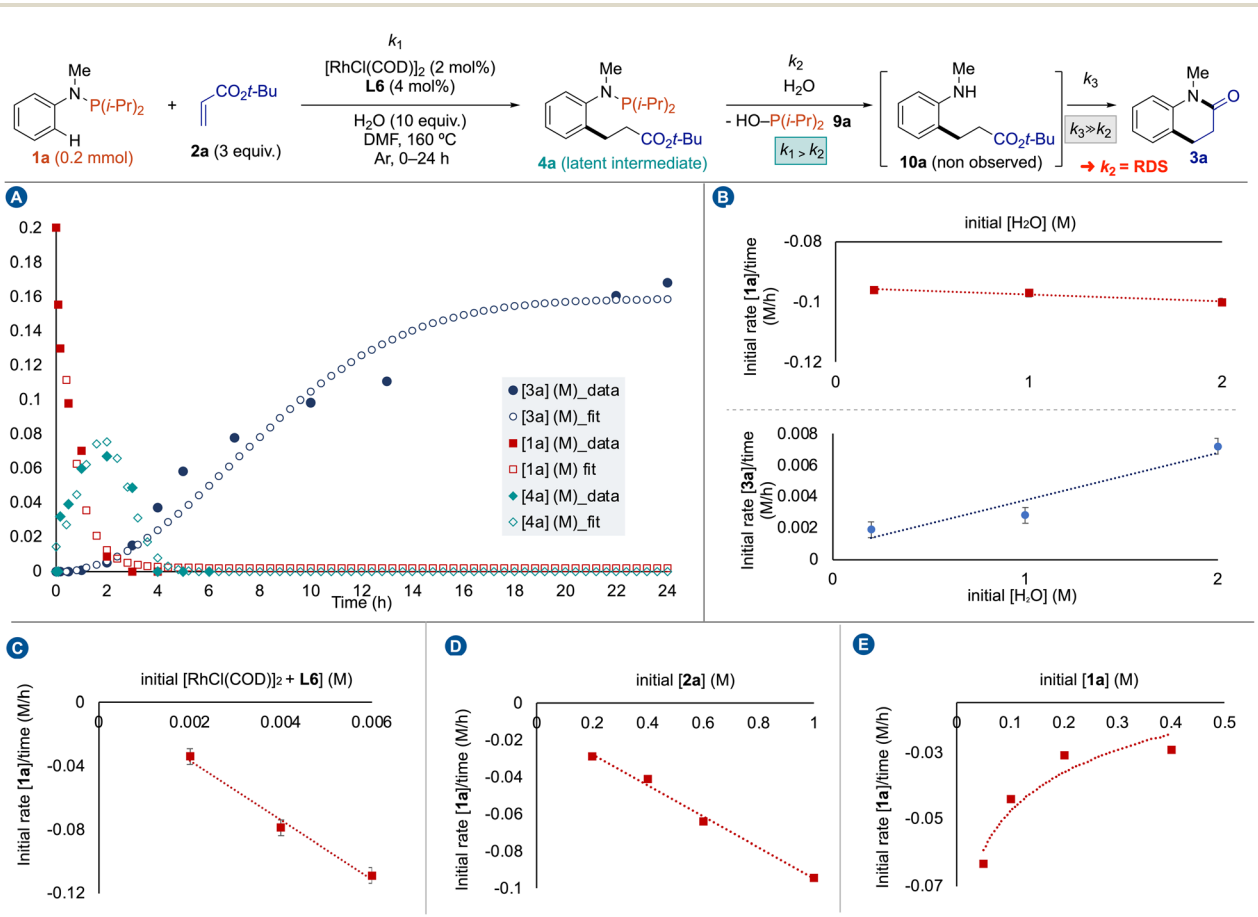

Fig. 3 Kinetic study: (A) reaction profile, (B) determination of H_2O order, (C) determination of catalyst order, (D) determination of **2a** order, (E) determination of **1a** order.

Then, we conducted a kinetic study to obtain a better picture of the reaction pathway (Fig. 3). First, we plotted the kinetic profile of the reaction by following the consumption of **1a**, the production and consumption of **4a** by ^{31}P NMR, while the production of **3a** was followed by ^{1}H NMR (Fig. 3A). The Gaussian-shape kinetic profile of **4a** indicates that $k_1 > k_2$ meaning that **4a** is a latent intermediate of the reaction. However, we have never observed hydrolyzed aniline **10a** during the reaction, possibly due to a spontaneous cyclization affording **3a**. Some *de facto* approximations were formulated. If [**10a**] ≈ 0 during the reaction, then $k_3 \gg k_2$; steps 2 and 3 can be considered as a single operation, and the rate determining step (RDS) is the hydrolysis of N–P(i-Pr)$_2$ bond. Our attention next turned toward determining the factors influencing the kinetic efficiency of Rh(I)-catalyzed cascade C(sp^2)–H bond alkylation – amidation of anilines. Reaction progress kinetic analysis revealed that catalyst deactivation was not caused by substrates or product formation, including **9a**.[17] Then, we measured the initial reaction rate for the model reaction as a function of the concentration of water, catalyst, *tert*-butylacrylate (**2a**) and phosphanamine **1a** in DMF at 160 °C. Interestingly, we observed a zero-order dependence on water for the consumption of **1a**, and a first-order dependence for the production of **3a** (Fig. 3B). These observations indicate that the water is required for the second step, namely the hydrolysis of N–P(i-Pr)$_2$ bond, and its presence (up to 10 equivalents) has a negligible influence on the Rh(I) catalytic activity.[23] In contrast, first-order dependence on Rh/**L6** catalytic system was observed for the consumption of **1a** (Fig. 3C). The first-order dependence of the reaction rate on acrylate concentration was obtained from the linear plot of initial rate (Δ[**1a**]/Δ*t*) *vs.* initial acrylate concentration ([**2a**]) (Fig. 3D). Saturation kinetics were observed with respect to phosphanamine concentration ([**1a**]) when similar experiments were carried out by measuring the initial rate over a range of **1a** concentrations (Fig. 3E). This rate inhibition by phosphanamine **1a** might have been anticipated due the strong ability of P(III)-ligands to coordinate Rh delivering a fully-coordinate stable complexes as resting state catalysts.

Based on our mechanistic and kinetic investigations and the DFT calculation by Bai, Lan on Rh(I)-catalyzed C7-alkylation of indole N–P*t*-Bu$_2$ [24] – which demonstrated that μ_2-bridged dinuclear rhodium complexes preferentially act as active catalysts because of the endothermic monomerization process – we propose the catalytic cycle depicted in Fig. 4. [RhCl(COD)]$_2$ complex reacts with phosphanamine **1a** to form the active catalytic species **I**. Then, oxidative addition occurs to deliver the Rh(III)–H hydride **II**. Acrylate **2a** may followed by 1,2-insertion to yield **III**. Then, reductive elimination affords **IV**. In the presence of water, the coordinated functionalized phosphanamine is prompted to hydrolysis to give the desired product **3a** along with Rh complex **V** surrounded by hydroxydiisopropylphosphane (**9a**). The next catalytic cycle starts by a ligand exchange between **9a** and **1a** to give **I**. However, **V** or **I** may react with phosphine derivatives **9a** or **1a** in an inhibitory manner to form nonproductive coordination complexes [{Rh(**9a**)$_2$(μ_2-Cl)}$_2$] and [{Rh(**1a**)$_2$(μ_2-Cl)}$_2$]. At this stage, the exact role of **L6** remains unclear but it may help the decomplexation of one phosphine to regenerate the active catalysts.

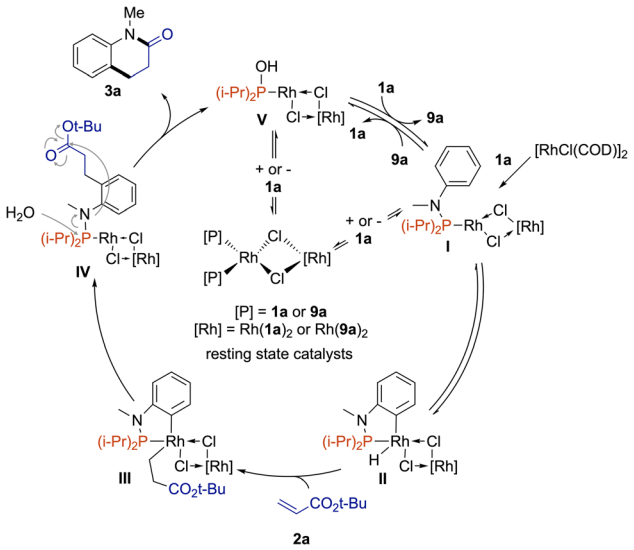

Fig. 4 Proposed mechanism.

Conclusions

We have developed a novel method for the construction of functionalized dihydroquinolinone scaffolds based on a cascade reaction of Rh(I)-catalyzed C(sp^2)–H bond functionalization of phosphanamines with acrylates followed by N–P hydrolysis and intramolecular amidation. The reaction features good substrate scope with respect to both coupling partners. A mechanistic investigation established a viable catalytic cycle that was consistent with the kinetic data obtained and revealed that P(III)-directed C(sp^2)–H bond functionalization with Rh(I) occurred through oxidative addition leading to Rh–H species and an inhibitory effect by the trivalent phosphorus species. The formal C(sp^2)–H bond alkylation of anilines was also extended to styrene derivatives to afford the corresponding *ortho*-alkylated anilines. Finally, the utility of this protocol was demonstrated by the synthesis of aripiprazole *N*-methylated analog from easily accessible and cheap *N*-methylaniline. These findings provide a general framework for improving and expanding the scope of Rh(I)-catalyzed C(sp^2)–H bond activation in synthetic organic chemistry of *N*-heterocycles, and the collected mechanistic insights should benefit in the future development of Rh(I)-catalyzed P(III)-directed C–H bond activation.

Data availability

General information, detailed experimental procedures, kinetics, characterization data for all new compounds, and NMR spectra are in the ESI.†

Author contributions

M. P. co-conceived, performed the laboratory experiments (optimization, substrate scope, application and mechanistic studies) and analyzed the experimental data. D. A. performed the laboratory experiments for substate scope. T. R. did the X-

ray analysis. H.-D. took part to the discussions and proofread the manuscript. J.-F. S. conceived, directed the investigations, analyzed the experimental data, and prepared the manuscript.

Conflicts of interest

There are no conflicts to declare.

Acknowledgements

We thank the CNRS, UR1, Agence Nationale de la Recherche (Grant No. ANR-20-CE07-0019-01) for providing financial support, and Rennes 1 University for PhD grant to M. Peng. We thank Umicore AG & Co. KG for their generous donation of rhodium(III) chloride hydrate.

Notes and references

1 (*a*) J. Fischer and C. R. Ganellin, *Analogue-based Drug Discovery*, John Wiley & Sons, Weinheim, 2006; (*b*) R. Sharma, R. K. Yadav, R. Sharma, N. K. Sahu, M. Jain and S. Chaudhary, *Curr. Top. Med. Chem.*, 2021, **21**, 1538–1571.

2 (*a*) M. Cherest and X. Lusinchi, *Tetrahedron Lett.*, 1989, **30**, 715–718; (*b*) M. C. Elliott and S. V. Wordingham, *Synlett*, 2004, 898–900; (*c*) K. Li, L. N. Foresee and J. A. Tunge, *J. Org. Chem.*, 2005, **70**, 2881–2883.

3 (*a*) M. Wasa and J.-Q. Yu, *J. Am. Chem. Soc.*, 2008, **130**, 14058–14059; (*b*) L. Zhang, L. Sonaglia, J. Stacey and M. Lautens, *Org. Lett.*, 2013, **15**, 2128–2131; (*c*) J.-X. Yan, H. Li, X.-W. Liu, J.-L. Shi, X. Wang and Z.-J. Shi, *Angew. Chem., Int. Ed.*, 2014, **53**, 4945–4949; (*d*) B. Li, Y. Park and S. Chang, *J. Am. Chem. Soc.*, 2014, **136**, 1125–1131; (*e*) M. Guan, Y. Pang, J. Zhang and Y. Zhao, *Chem. Commun.*, 2016, **52**, 7043–7046; (*f*) Z. Kuang, B. Li and Q. Song, *Chem. Commun.*, 2018, **54**, 34–37; (*g*) H.-Z. Xiao, W.-S. Wang, Y.-S. Sun, H. Luo, B.-W. Li, X.-D. Wang, W.-L. Lin and F.-X. Luo, *Org. Lett.*, 2019, **21**, 1668–1671.

4 (*a*) T. E. Hurst, R. M. Gorman, P. Drouhin, A. Perry and R. J. K. Taylor, *Chem.–Eur. J.*, 2014, **20**, 14063–14073; (*b*) Q.-F. Bai, C. Jin, J.-Y. He and G. Feng, *Org. Lett.*, 2018, **20**, 2172–2175; (*c*) H. Cheng, T.-L. Lam, Y. Liu, Z. Tang and C.-M. Che, *Angew. Chem., Int. Ed.*, 2021, **60**, 1383–1389; (*d*) Z. Liu, S. Zhong, X. Ji, G.-J. Deng and H. Huang, *Org. Lett.*, 2022, **24**, 349–353.

5 (*a*) T.-P. Loh and L.-L. Wei, *Synlett*, 1998, **1**, 975–976; (*b*) C. Munro-Leighton, E. D. Blue and T. B. Gunnoe, *J. Am. Chem. Soc.*, 2006, **128**, 1446–1447; (*c*) K. De, J. Legros, B. Crousse and D. Bonnet-Delpon, *J. Org. Chem.*, 2009, **74**, 6260–6265.

6 J. Wu, S. Xiang, J. Zeng, M. Leow and X.-W. Liu, *Org. Lett.*, 2015, **17**, 222–225.

7 X. Liu and K. K. Hii, *J. Org. Chem.*, 2011, **76**, 8022–8026.

8 J. Kim, S.-W. Park, M.-H. Baik and S. Chang, *J. Am. Chem. Soc.*, 2015, **137**, 13448–13451.

9 J. Chen, G. Song, C.-L. Pan and X. Li, *Org. Lett.*, 2010, **12**, 5426–5429.

10 (*a*) J. Qi, L. Huang, Z. Wang and H. Jiang, *Org. Biomol. Chem.*, 2013, **11**, 8009–8013; (*b*) S. M. Khake and N. Chatani, *ACS Catal.*, 2022, **12**, 4394–4401.

11 (*a*) Q. Shelby, N. Kataoka, G. Mann and J. Hartwig, *J. Am. Chem. Soc.*, 2000, **122**, 10718–10719; (*b*) X. Qiu, M. Wang, Y. Zhao and Z. Shi, *Angew. Chem., Int. Ed.*, 2017, **56**, 7233–7237; (*c*) X. Luo, J. Yuan, C.-D. Yue, Z.-Y. Zhang, J. Chen, G.-A. Yu and C.-M. Che, *Org. Lett.*, 2018, **20**, 1810–1814; (*d*) X. Qiu, H. Deng, Y. Zhao and Z. Shi, *Sci. Adv.*, 2018, **4**, eaau6468; (*e*) K. Fukuda, N. Iwasawa and J. Takaya, *Angew. Chem., Int. Ed.*, 2019, **58**, 2850–2853; (*f*) J.-W. Li, L.-N. Wang, M. Li, P.-T. Tang, X.-P. Luo, M. Kurmoo, Y.-J. Liu and M.-H. Zeng, *Org. Lett.*, 2019, **21**, 2885–2889; (*g*) D. Wang, Y. Zhao, C. Yuan, J. Wen, Y. Zhao and Z. Shi, *Angew. Chem., Int. Ed.*, 2019, **58**, 12529–12533; (*h*) J. Wen, D. Wang, J. Qian, D. Wang, C. Zhu, Y. Zhao and Z. Shi, *Angew. Chem., Int. Ed.*, 2019, **58**, 2078–2082; (*i*) S. E. Wright, S. Richardson-Solorzano, T. N. Stewart, C. D. Miller, K. C. Morris, C. J. A. Daley and T. B. Clark, *Angew. Chem., Int. Ed.*, 2019, **58**, 2834–2838; (*j*) B. Dong, J. Qian, M. Li, Z.-J. Wang, M. Wang, D. Wang, C. Yuan, Y. Han, Y. Zhao and Z. Shi, *Sci. Adv.*, 2020, **6**, eabd1378; (*k*) Y. Homma, K. Fukuda, N. Iwasawa and J. Takaya, *Chem. Commun.*, 2020, **56**, 10710–10713; (*l*) G. Li, J. An, C. Jia, B. Yan, L. Zhong, J. Wang and S. Yang, *Org. Lett.*, 2020, **22**, 9450–9455; (*m*) Z. Shi, M. Wang, H. Luo and D. Wang, *Synlett*, 2020, **33**, 351–356; (*n*) J. Wen, B. Dong, J. Zhu, Y. Zhao and Z. Shi, *Angew. Chem., Int. Ed.*, 2020, **59**, 10909–10912; (*o*) Z. Zhang, M. Cordier, P. H. Dixneuf and J.-F. Soulé, *Org. Lett.*, 2020, **22**, 5936–5940; (*p*) Z.-Y. Zhang, X. Zhang, J. Yuan, C.-D. Yue, S. Meng, J. Chen, G.-A. Yu and C.-M. Che, *Chem.–Eur. J.*, 2020, **26**, 5037–5050; (*q*) T. Komuro, J. Asagami, H. Higashi, K. Sato, H. Hashimoto and H. Tobita, *Organometallics*, 2021, **40**, 3113–3123; (*r*) M. Li, J.-Y. Tao, L.-N. Wang, J.-W. Li, Y.-J. Liu and M.-H. Zeng, *J. Org. Chem.*, 2021, **86**, 11915–11925; (*s*) L.-N. Wang, P.-T. Tang, M. Li, J.-W. Li, Y.-J. Liu and M.-H. Zeng, *Adv. Synth. Catal.*, 2021, **363**, 2843–2849; (*t*) H.-B. Xu, Y.-J. Chen, X.-Y. Chai, J.-H. Yang, Y.-J. Xu and L. Dong, *Org. Lett.*, 2021, **23**, 2052–2056; (*u*) N.-J. Zhang, W.-T. Ma, J.-W. Li, Y.-J. Liu and M.-H. Zeng, *Asian J. Org. Chem.*, 2021, **10**, 1113–1116; (*v*) Y. Fu, C.-H. Chen, M.-G. Huang, J.-Y. Tao, X. Peng, H.-B. Xu, Y.-J. Liu and M.-H. Zeng, *ACS Catal.*, 2022, **12**, 5036–5047; (*w*) W.-T. Ma, M.-G. Huang, Y. Fu, Z.-H. Wang, J.-Y. Tao, J.-W. Li, Y.-J. Liu and M.-H. Zeng, *Chem. Commun.*, 2022, **58**, 7152–7155; (*x*) D. Wang, M. Li, C. Shuang, Y. Liang, Y. Zhao, M. Wang and Z. Shi, *Nat. Commun.*, 2022, **13**, 2934.

12 (*a*) X. Qiu, P. Wang, D. Wang, M. Wang, Y. Yuan and Z. Shi, *Angew. Chem., Int. Ed.*, 2019, **58**, 1504–1508; (*b*) A. J. Borah and Z. Shi, *J. Am. Chem. Soc.*, 2018, **140**, 6062–6066.

13 (*a*) Z. Zhang, T. Roisnel, P. H. Dixneuf and J.-F. Soulé, *Angew. Chem., Int. Ed.*, 2019, **58**, 14110–14114; (*b*) J.-W. Li, L.-N. Wang, M. Li, P.-T. Tang, N.-J. Zhang, T. Li, X.-P. Luo, M. Kurmoo, Y.-J. Liu and M.-H. Zeng, *Org. Lett.*, 2020, **22**, 1331–1335; (*c*) D. Wang, B. Dong, Y. Wang, J. Qian, J. Zhu, Y. Zhao and Z. Shi, *Nat. Commun.*, 2019, **10**, 3539.

14 (*a*) D. L. Davies, S. M. A. Donald and S. A. Macgregor, *J. Am. Chem. Soc.*, 2005, **127**, 13754–13755; (*b*) D. A. Colby, R. G. Bergman and J. A. Ellman, *Chem. Rev.*, 2010, **110**, 624–655.

15 Reaction of 1,1-diisopropyl-*N*-phenylphosphanamine with **2a** resulted in *N*-addition reaction.

16 (*a*) M. A. Grady, T. L. Gasperoni and P. Kirkpatrick, *Nat. Rev. Drug Discovery*, 2003, **2**, 427–428; (*b*) V. Ozdemir, J. Fourie and F. Ozdener, *Curr. Opin. Investig. Drugs*, 2002, **3**, 113–120.

17 P. Kowalski, J. Jaskowska and Z. Majka, *Mini-Rev. Org. Chem.*, 2012, **9**, 374–380.

18 S. J. Bonacorsi Jr, S. C. Waller and J. Kent Rinehart, *J. Label. Compd. Radiopharm.*, 2006, **49**, 1–9.

19 See ESI for more details.†

20 (*a*) R. B. Bedford, S. J. Coles, M. B. Hursthouse and M. E. Limmert, *Angew. Chem., Int. Ed.*, 2003, **42**, 112–114; (*b*) R. B. Bedford, M. Betham, A. J. M. Caffyn, J. P. H. Charmant, L. C. Lewis-Alleyne, P. D. Long, D. Polo-Cerón and S. Prashar, *Chem. Commun.*, 2008, 990–992.

21 K. Wang, G. P. Rosini, S. P. Nolan and A. S. Goldman, *J. Am. Chem. Soc.*, 1995, **117**, 5082–5088.

22 B. Rybtchinski, R. Cohen, Y. Ben-David, J. M. L. Martin and D. Milstein, *J. Am. Chem. Soc.*, 2003, **125**, 11041–11050.

23 We have also demonstrated that **1a** is stable in the presence of 2 mol% $[RhCl(COD)]_2$ associated with 4 mol% of **L6**, and 10 equivalents of water in DMF over several hours, suggesting that N–P bond hydrolysis majority occurs on the complexed phosphanamines.

24 D. Heng, H. Chen, X. He, S. Liu, L. Zhu, K. Zhong, T. Zhang, R. Bai and Y. Lan, *ACS Catal.*, 2021, **11**, 3975–3987.